Title :	Assessment of the impact of a 10'' HEW PSF on the possibility to investigate star-forming regions and OB associations in the Milky Way and the Magellanic Clouds under SWG3.2		
Date:	2022-02-23	Issue:	2.0
Reference:	SWG3.2-TN-0008		

Authors :		Date :
S. Sciortino	INAF - Osservatorio Astronomico di Palermo, Italy	
G. Rauw	Liège University, Belgium	
Y. Nazé	Liège University, Belgium	
Contributors :		
N. Grosso	Laboratoire d'Astrophysique de Marseille, France	
J. Mackey	Dublin Institute for Advanced Studies, Ireland	
I. Pillitteri	INAF - Osservatorio Astronomico di Palermo, Italy	
A. Pollock	University of Sheffield, United Kingdom	
J. Robrade	Hamburger Sternwarte, Germany	
S. Wolk	CXC Harvard-Smithonian CfA, USA	

CHANGES LOG

Issue	Date	Modifications
0.1	2022-01-31	First draft
1.0	2022-02-04	Addition of SIXTE simulations
1.1	2022-02-08	Update of SIXTE simulations
1.2	2022-02-09	Version distributed to ASST chair and SWG 3.2
2.0	2022-02-23	Correction of TN number. Version submitted to ASST after SWG 3.2 comments

Table of contents

1 REFERENCES

1.1 REFERENCE DOCUMENTS

Title	**Reference**
The Hot and Energetic Universe: Star formation and evolution (Sciortino, S., Rauw, G., Audard, M., et al. 2013, arXiv:1306.2333)	RD1

1.2 APPLICABLE DOCUMENTS

Title of the Document	Reference
Athena Mock Observation Plan (v4.1)	AD1

1.3 ACRONYMS

Abbr.	Signification
ASST	*Athena* Science Study Team
FoV	Field of view
FWHM	Full Width at Half Maximum
HEW	Half Energy Width
MOP	Mock Observation Plan [AD1]
SFR	Star Forming Region
TN	Technical Note
WFI	Wide Field Imager
WG	Working Group
X-IFU	X-ray Integral Field Unit

2 INTRODUCTION

ASST asked the *Athena* Working Groups and Topical Panels to assess the impact of a 10'' HEW for the *Athena* mirrors on the different science topics. Among the science objectives of *SWG 3.2 Star formation and Evolution* as formulated in [RD1], R.SCOBJ-322 deals with colliding wind interactions in massive binaries, R.SCIOBJ-323 aims at the study of pre-main sequence stars in Galactic star-forming regions, and R.SCIOBJ-325 aims at a better understanding of the relationship between the stellar winds of massive stars and their X-ray emission.

Whilst the targets for R.SCIOBJ-322 in the *Athena* mock observing plan [AD1] mostly concern rather isolated sources, many colliding wind binaries that could become targets for studies with Athena are located in clusters (e.g. Arora & Pandey 2020), and source confusion and cross contamination of source spectra becomes a limiting factor in those cases.

Regarding R.SCIOBJ-323 the *Athena* mock observing plan [AD1] lists three 50 ks observations of the Orion central region, of IC 348 and of Cha I. One of the main objectives of those observations is to reach a deep limiting sensitivity over an area much wider than the one explored so far with the specific purpose of studying the X-ray emission of young very-low mass stars and brown dwarfs, in order to help discriminating the mechanism, e.g. diffuse dynamos vs. aurora-like process, that generates their X-ray emission.

One of the key questions of R.SCIOBJ-325 is to investigate the L_X/L_{bol} relation of OB stars at lower than solar metallicity. Theoretical models predict that the winds at lower metallicity should be weaker and as a result, one would expect also intrinsically lower X-ray emission, though the attenuation by photoelectric absorption in the stellar wind itself would also be reduced. The *Athena* MOP [AD1] hence includes three WFI observations of Magellanic Cloud regions hosting OB associations. The targets selected for this purpose are N11 and N44 in the LMC and NGC 371 in the SMC. Each region should be observed for 100 ks with the goal to characterize the emission from individual massive stars.

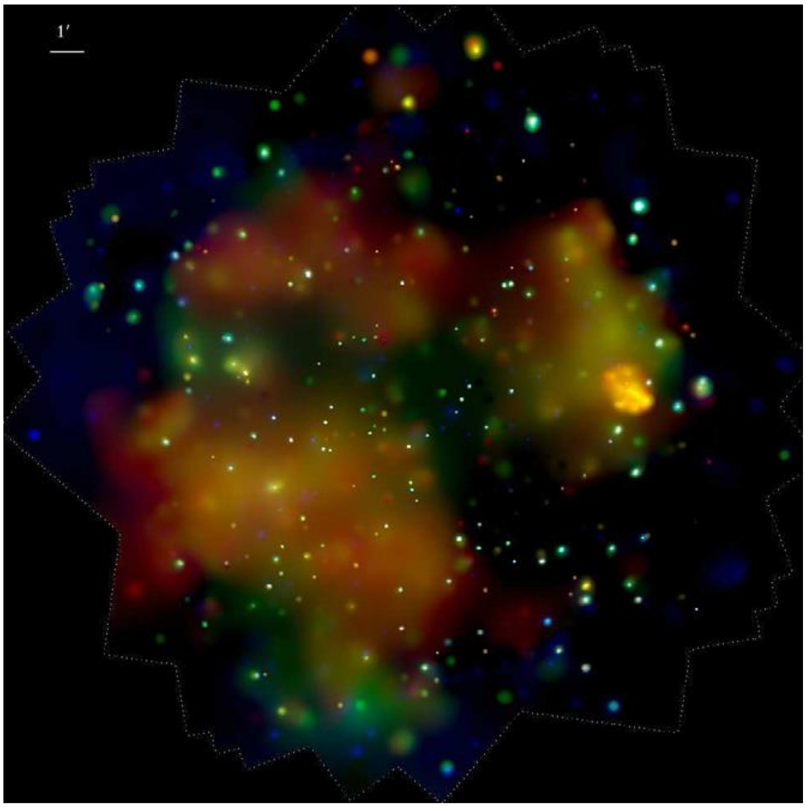

Figure 1 : Three-colour mosaic of the *Chandra* images of N11 (Nazé et al. 2014). The red, green and blue colours correspond to the 0.5 – 2, 2 – 4, and 4 – 8 keV energy bands.

N11 has been observed previously with *XMM-Newton* (30 ks, Nazé et al. 2004) and *Chandra* (300 ks, Nazé et al. 2014, see Fig.1). The *Chandra* observation allowed the detection of about a dozen individual sources associated with OB stars with X-ray fluxes down to about 10^{-15} erg cm^{-2} s^{-1}. These detections likely constitute only the tip of the iceberg, i.e. the X-ray brightest objects possibly associated with colliding wind binary systems or magnetic massive stars. The goal of the proposed *Athena* observations is to go significantly deeper. It has to be stressed here that the N11 region hosts a significant diffuse X-ray emission as revealed by Fig.1 (Nazé et al. 2014). A very similar situation most likely applies to N44 and NGC 371.

In this TN, we investigate the impact of a 10'' HEW PSF on the feasibility and science return of the proposed Athena WFI observations of crowded SFRs and OB associations in the Magellanic Clouds.

3 THE IMPACT OF A 10" HEW PSF ON OBSERVATIONS OF MAGELLANIC CLOUDS O-STARS

3.1 *ATHENA* WFI SENSITIVITY

Figure 2 (from Evans et al. 2006) illustrates an optical image of the N11 region. OB-type stars are mostly concentrated in a few young open clusters (LH9, LH10, LH13). Here we focus on those stars that were classified as O-type stars (i.e. hotter than 30 kK) in the LH9 and LH10 clusters according to the study of Parker et al. (1992).

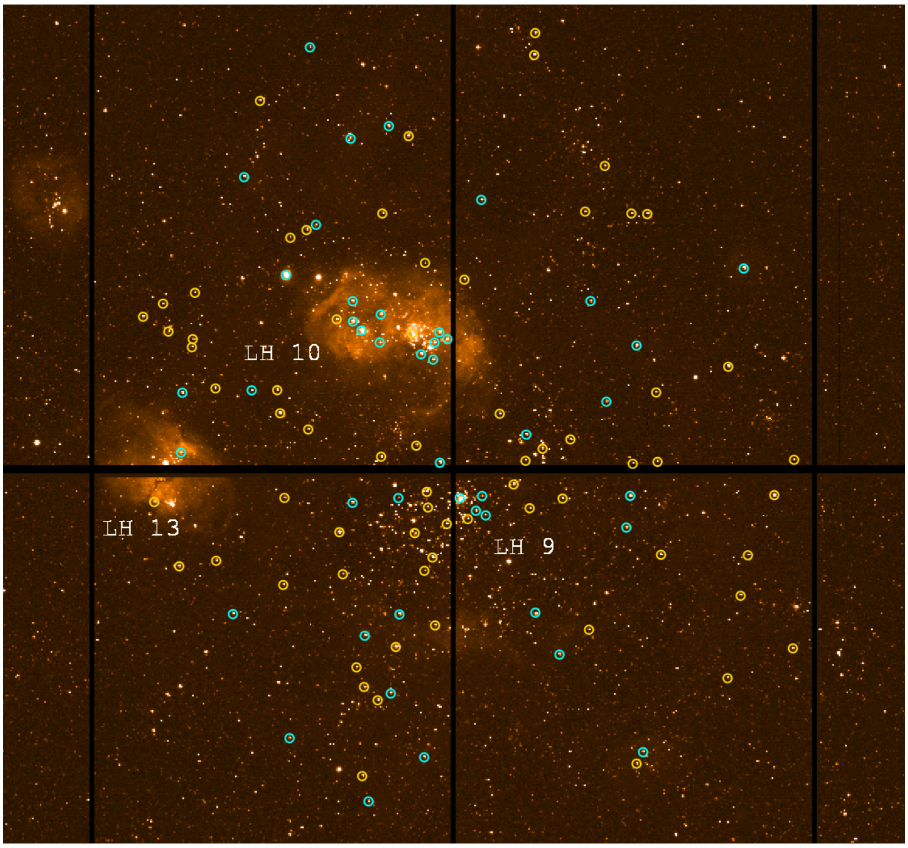

Figure 2: Optical image of the N11 region (Evans et al. 2006).

Figure 3 illustrates a histogram of the expected X-ray fluxes assuming the same $L_X/L_{bol} = 10^{-7}$ relation as found for Galactic O-type stars and applied to O-stars in N11 (Parker et al. 1992) and N44 (Oey & Massey 1995). As pointed out above, some of the objects that were previously detected with Chandra could be X-ray over-luminous (due to colliding wind interactions and/or magnetic wind confinement). Such effects are not taken into account here. We have then assumed a flux detection limit (within 100 ks) of about 1.6 10^{-16} erg cm^{-2} s^{-1} (i.e. 10^{-3} WFI cts s^{-1}) for a 5'' HEW PSF. A 10'' HEW PSF would degrade the sensitivity by about a factor ~1.5 to 2.4 × 10^{-16} erg cm^{-2} s^{-1}. These numbers are motivated by the results of detailed SIXTE simulations done for the NGC 2264 and ρ Oph SFRs (see below). Hence not all individual O-type stars in these OB associations will be detectable with *Athena* even with a 5'' PSF. For a 5'' HEW PSF, 44 objects (out of 116) in N11 and 23 objects (out of 36) in N44 would be within reach of the *Athena* WFI. For a 10'' HEW PSF, these numbers drop to 31 and 11 for N11 and N44, respectively. This reduction however only accounts (to zeroth order) for the loss in sensitivity due to the smearing out of the source photons over a wider area. Further losses are expected due to source crowding and a lower contrast against the diffuse emission.

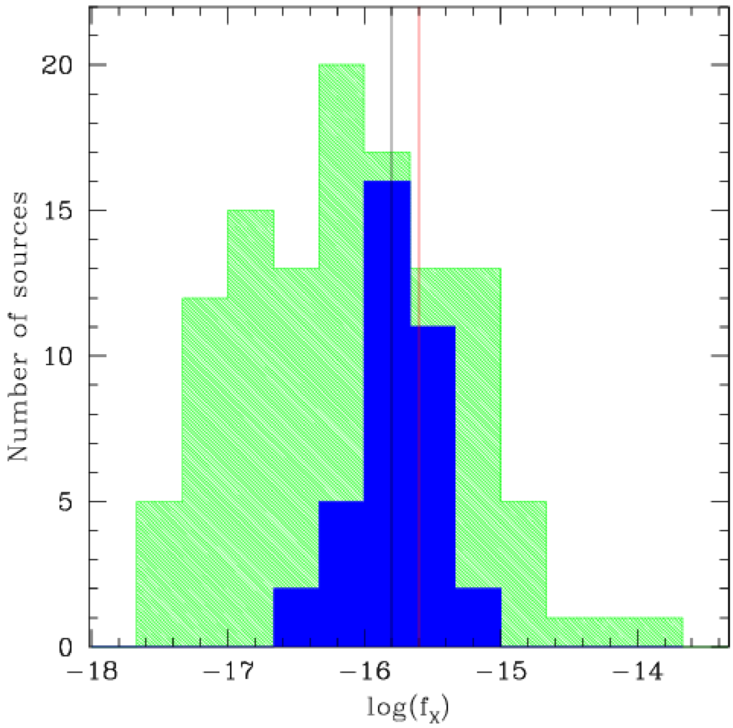

Figure 3: Expected X-ray fluxes of 116 O-type stars in N11 (green histogram) and 36 O-type stars in N44 (blue histogram). The vertical lines correspond to the expected sensitivity for a 5'' HEW PSF (black line) or a 10'' HEW PSF (red line).

3.2 SOURCE CROWDING

Figure 4 and 5 illustrate the positions of those O-type in N11 and N44. The symbols have a circular shape with a radius of 5'' on the left and 10'' on the right[1]. Objects with fluxes above the detection threshold are displayed as filled blue circles. Whilst the most crowded parts of LH10 (the cluster which is farther to the North in the N11 field) are unresolved even at 5'', we clearly see the severe source confusion that appears at 10'': the number of individually resolvable sources decreases from ~31 to 15 (i.e. a similar number of objects as already detected by *Chandra*). At 10'' HEW, the vast majority of the sources in LH9 (the cluster to the South) are also blended, leading to cross-contamination of their spectra and photometry by neighbouring sources. A further degradation of the capability to resolve individual sources will come from the proximity of unresolved sources that have individual fluxes below the detection threshold (the white circles in Figs. 4 and 5). The situation is slightly better for N44 (see Fig. 5), mostly because of a considerably lower number

---

[1] Here we use 5'' and 10'' radii (instead of diameters) as source counts will spread over the entire PSF, i.e. beyond its narrow core, and thus cross-contaminate the signal from neighbouring sources.

of O-type stars in this association. In this case, source crowding should not lead to a significant effect on the number of detectable objects.

More generally speaking, source crowding will also affect observations of the star forming regions in the Galaxy. Based on available *Chandra*-ACIS X-ray data it is obvious that the central region of Orion will be too crowded even for the 5'' HEW PSF, but the outer regions can be investigated with that PSF. Instead, the 10'' HEW PSF will significantly reduce the scientific return of a WFI observation of Orion. In order to investigate possible alternative targets and the effect of a wider PSF on SFR less crowded than Orion, we have selected NGC 2264 that has been observed for 100 ks with *Chandra* ACIS finding a bit more than 1000 sources. This region has been the subject of a dedicated set of simulations (see below) that permitted to predict the attainable limiting sensitivity and to better quantify the effect of confusion due to the increase of PSF width.

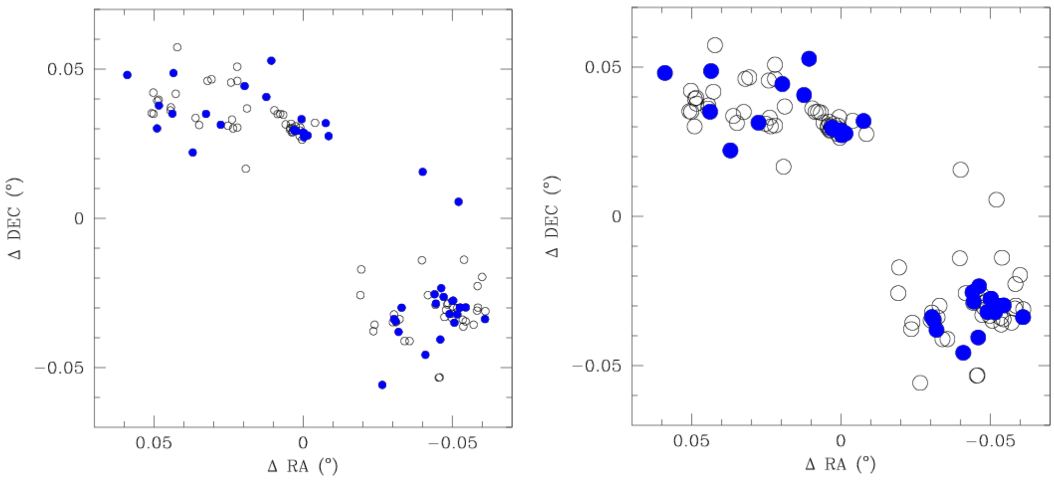

Figure 4: Distribution of O-type stars in the LH9 and LH10 clusters of the N11 region. On the left the symbols have a radius of 5'', whilst the radius is 10'' on the right. The positions of the sources are taken from Parker et al. (1992). Open circles stand for sources below the detection threshold, whereas blue filled circles indicate sources that are expected to be brighter than the detection limit.

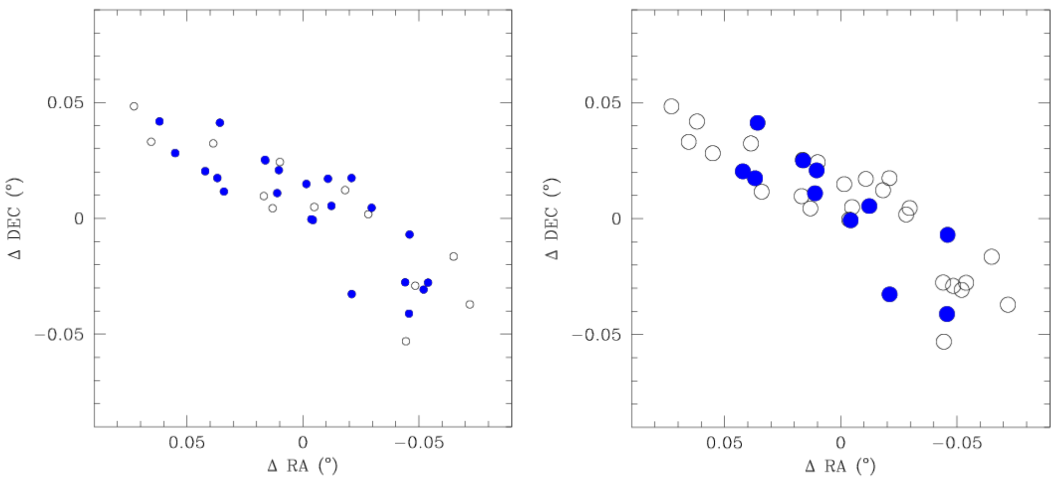

Figure 5: Same as Fig. 4, but for the N44 region. The positions of the sources are taken from Oey & Massey (1995).

Another aspect that will be significantly impacted by source crowding is the study of the diffuse X-ray emission in SFRs. Such studies are important to assess the feedback from massive stars into the interstellar medium (e.g. Rosen et al. 2014). A 10'' HEW PSF will lead to more unresolved source, thus making it significantly more difficult to distinguish genuine diffuse emission from unresolved sources.

3.3 THE IMPACT OF THE DIFFUSE EMISSION

As pointed out above, N11 features diffuse X-ray emission (part of which comes from genuine wind-blown (super)bubbles, part of which is due to a population of unresolved pre-main-sequence stars). To investigate the impact of this diffuse emission, we have used the spectrum of the diffuse emission extracted over a circular region of 29.5'' radius within LH9 as observed with *Chandra* ACIS (Nazé et al. 2014). The spectrum was fitted under xspec with a simple wabs*apec model (setting the metallicity of the plasma model to 0.3 solar, and performing the fit over the 0.3 – 2.0 keV energy band). The best fit column density was 0.45×10^{22} cm^{-2} with a best-fit plasma temperature of kT = 0.19 keV. The corresponding net ACIS count rate was 3.72×10^{-7} cts s^{-1} keV^{-1} $arcsec^{-2}$. Folding the best-fit model through the WFI response yields an expected rate of 2.88×10^{-5} cts s^{-1} keV^{-1} $arcsec^{-2}$, two orders of magnitude above the flat internal particle background of the WFI.

For a circular extraction region of 2.5'' radius, we thus expect a diffuse background contribution of 96 counts within an exposure time of 100 ks, and a 4 times higher contribution for a 10'' radius region. Assuming that the future detection algorithm will start by adjusting an overall background map, we then estimate the signal-to-noise ratio of a detection from the following equation

$$\frac{S}{N} = \frac{Net\ source\ counts}{\sigma shot}$$

where the noise terms in the denominator corresponds to the photon noise of the source + background.

A source with a flux of 10^{-15} erg cm^{-2} s^{-1} is expected to produce a total of 577 WFI counts in 100 ks (half of them falling into the 2.5'' radius region), and will thus result in a S/N of 14.7 for a 5'' HEW. If instead, we consider a 10'' HEW, then the S/N is reduced to 11.1. For a source flux of 2.0×10^{-16} erg cm^{-2} s^{-1}, the corresponding values are 115 WFI counts, and S/N = 5.1 for 5'' HEW versus S/N = 2.7 for 10'' HEW.

We thus conclude that, in case of a 10'' HEW PSF, the diffuse background will further limit our ability to successfully extract the X-ray emission of massive stars in Magellanic Cloud regions.

4 DEDICATED SIMULATIONS OF GALACTIC AND MAGELLANIC CLOUDS STAR-FORMING REGIONS

The above estimates were checked with dedicated simulations using SIXTE. These simulations include

- the contributions of the local astrophysical background and of the diffuse emission in the Magellanic Cloud derived from the LH9 region (as discussed above), both have been modeled as a uniform brightness emission across the WFI FoV, and
- the contribution of 1043 point-like sources whose characteristics have been derived from a 100 ks *Chandra* observation of the NGC 2264 SFR in the Galaxy (Flaccomio et al. 2006). The source fluxes are spread over the $f_X \sim 7 \times 10^{-17}$ to 10^{-12} erg s^{-1} cm^{-2} range. Their flux distribution, as derived from the Chandra observation, is shown in Fig. 6.

In performing the simulations, we considered the case in which the source fluxes are as measured with *Chandra*, as well as the case of the sources being 100 times weaker to match the X-ray luminosity distribution of the more distant sources in the Magellanic Clouds. For each of the two source input flux lists we have simulated the 5'' HEW PSF and the 10'' HEW PSF cases.

The simulated data have been searched for sources with a prototype version of the PWDetect code (Damiani et al. 1997a, 1997b) recently adapted by S. Sciortino to the WFI data. The adopted prototype version incorporates the PSF shape parameterized according to the most recent available ray-tracing prediction as computed by R. Willingale (see https://www.cosmos.esa.int/web/athena/resources-by-esa). The most notable characteristics of the PSF shape are its core that is significantly narrower than for a 2D Gaussian with the same HEW and its extended wings. The fraction of the source photons contained in the wings increases with HEW of the PSF: for a source spectrum peaking at about 1 keV the fraction for the 10'' HEW PSF is about 1.5 times higher than for the 5'' HEW PSF. If the sources are strong enough the narrow PSF core allows to detect sources even if they are close together. However, in those cases (as well as in the case of confusion among weak sources with small separations) the difficulty to properly determine the intensity of individual sources, given the fraction of source counts in the PSF wings, remains to be solved.

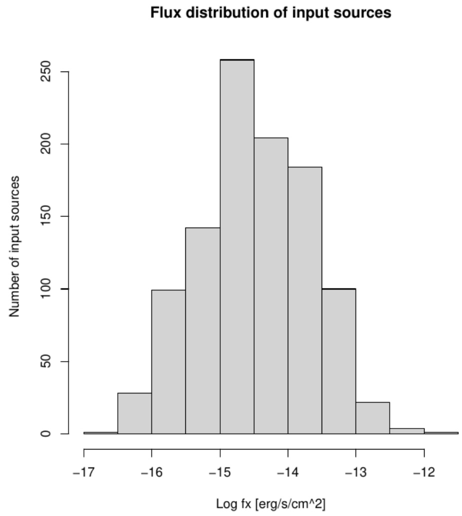

Figure 6: X-ray flux distribution of sources in NGC 2264 used in our SIXTE simulations.

Given the adopted detection acceptance threshold we expect no more than 1 – 2 false detections due to background fluctuations over the entire WFI FoV. For each of the 4 simulations, the positions of detected sources have been cross-correlated with the positions of the sources in the input source catalog assuming a separation of 2''. From the sample of all identifications we have searched the single ones. The results are summarized in the Table 1. In all cases, 1043 input sources have been simulated.

Table 1: Results of source detections in SIXTE simulations

Simulation	Detections	Single IDs	All IDs	Limiting f_X @ 50% area ($erg\ cm^{-2}\ s^{-1}$)
f_X as Chandra, 5'' HEW PSF	772	746	757	3×10^{-16}
f_X/100, 5'' HEW PSF	136	129	130	3×10^{-16}
f_X as Chandra, 10'' HEW PSF	609	569	577	6×10^{-16}
f_X/100, 10'' HEW PSF	66	54	54	6×10^{-16}

Considering the f_X/100 cases that are more representative of the planned WFI observations of Magellanic Cloud OB associations, it is evident that for the 10'' HEW PSF the number of detectable sources is reduced by a factor 2 while, in general, the attainable limiting sensitivity is reduced by nearly a factor 2.

Figures 7 and 8 illustrate the results of these simulations. Close inspection of the images (see Fig. 8) indicates that, as expected, weaker sources that are close together tend to "emerge" as an apparent single source, which will impact the identification of their optical counterpart. Whilst this effect is also present for a 5'' HEW, it becomes more severe at 10'' (see top row of Fig. 8).

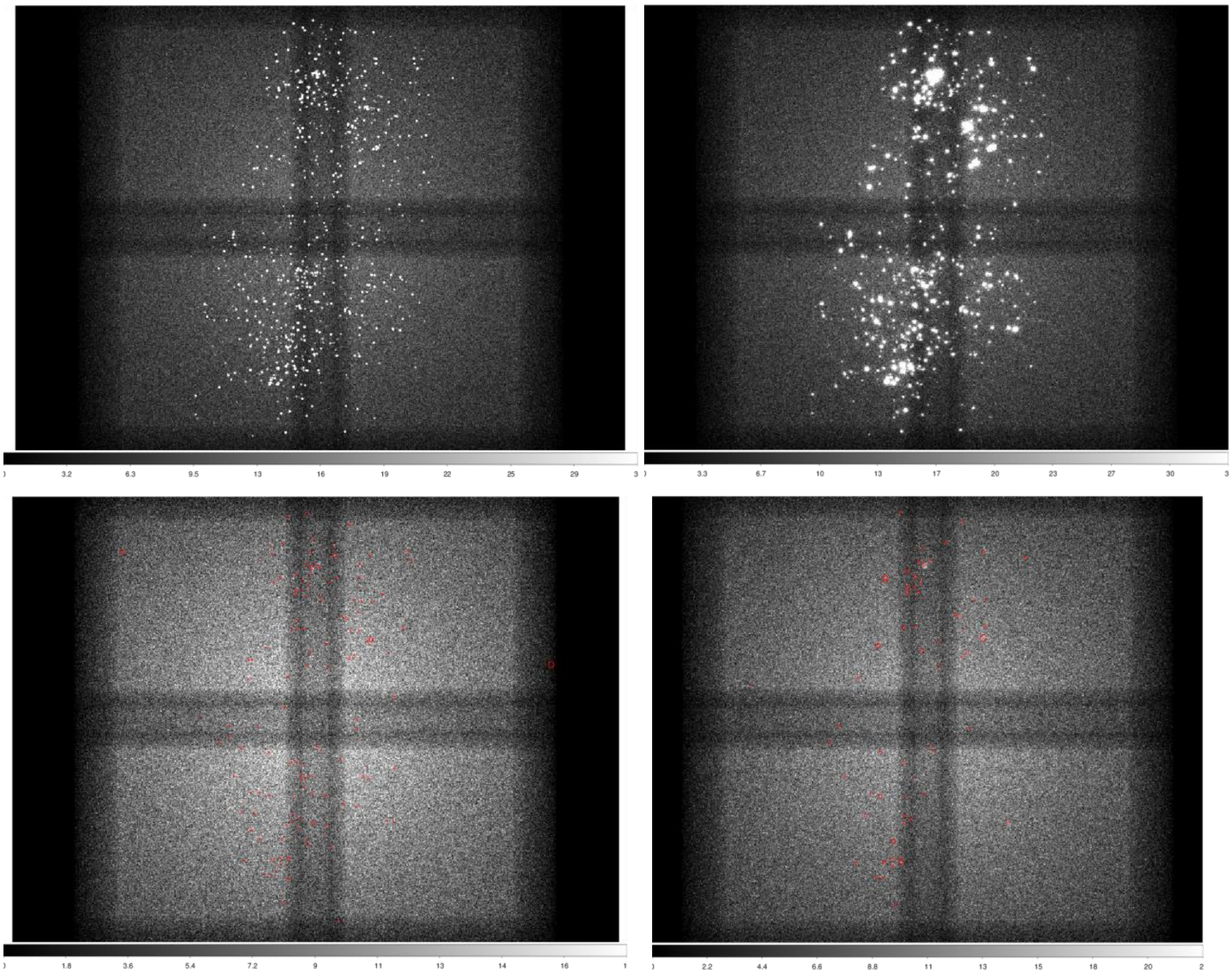

Figure 7: Simulated images of the NGC 2264 star-forming region. The images on the left correspond to a 5'' HEW, whilst those on the right are for a 10'' HEW. The top row corresponds to fluxes as observed, whilst the bottom row yields the case for fluxes divided by 100. Images are shown with a linear scale. In the bottom row, the locations of detected sources are shown by red circles.

5 CONCLUSIONS

In summary, as expected, going from a HEW of 5'' to 10'' has a tremendous impact on our ability to study crowded star-forming regions in our Galaxy and to investigate the dependence of the X-ray emission of massive stars on metallicity by studying individual sources in the Magellanic Clouds. Selecting targets with a lower source density can help, but at the expense of a much lower number of objects in the sample as most stellar groups in the MCs are quite dense. Isolated objects or stars in the periphery of the associations could be used, but are also few in number. This reduced sample size can probably not be easily compensated by increasing the number of regions to be investigated as other associations are as crowded and as impacted (or even worse so, e.g. 30 Dor in the LMC or NGC 3603 in our Galaxy) by diffuse emission, leading to a clear loss and bias of scientific results.

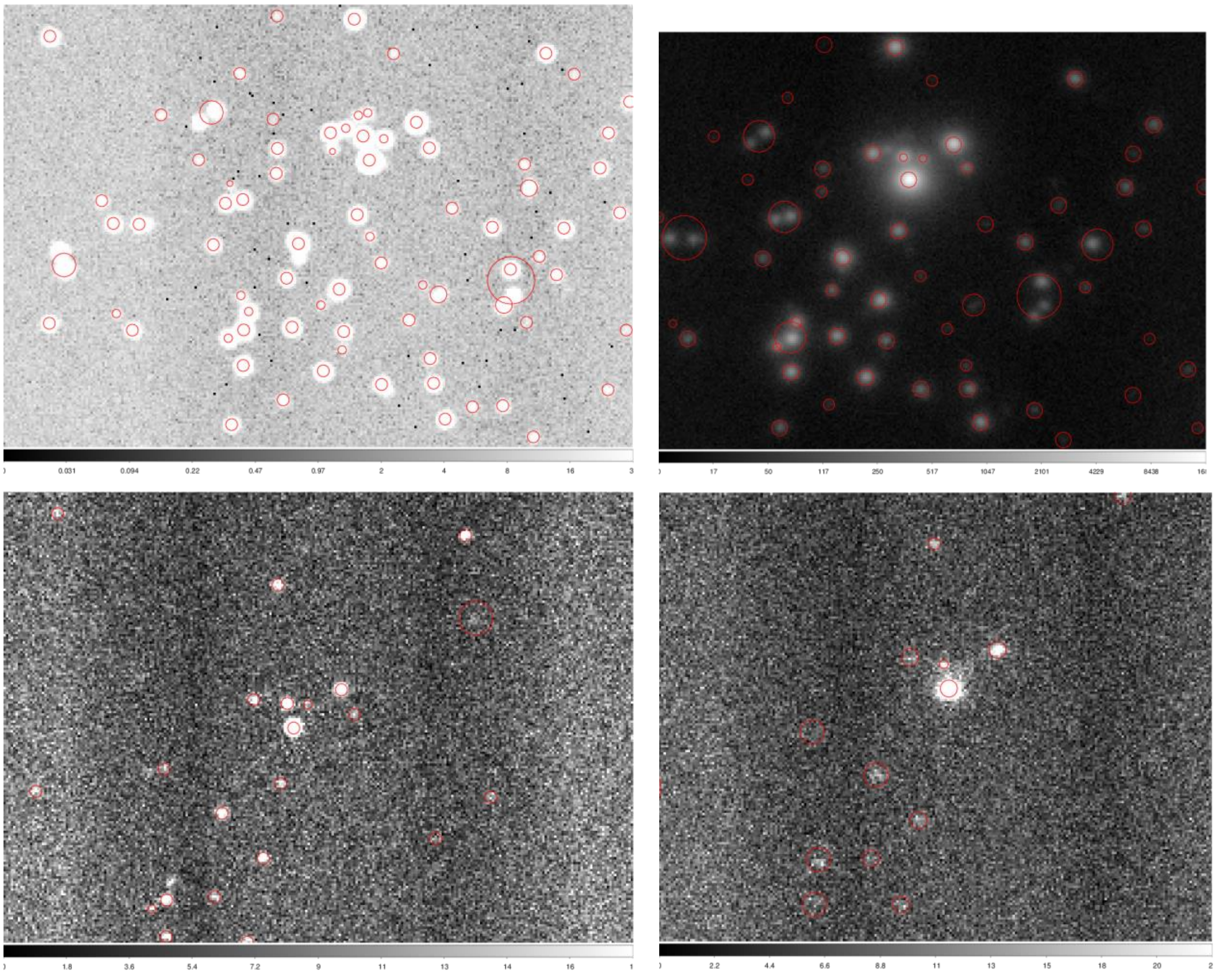

Figure 8: Zoom on some crowded regions of the simulated images of the NGC 2264 star-forming region. The top row illustrates the case of the fluxes as observed for 5'' HEW (left) and 10'' HEW (right). The bottom row illustrates the situation for fluxes divided by 100.

6 BIBLIOGRAPHY

- Arora, B., & Pandey, J.C. 2020, ApJ 891, 104
- Damiani, F., Maggio, A., Micela, G., & Sciortino, S. 1997a, ApJ 483, 350
- Damiani, F., Maggio, A., Micela, G., & Sciortino, S. 1997b, ApJ 483, 370
- Evans, C.J., Lennon, D.J., Smartt, S.J., Trundle, C. 2006, A&A 456, 623
- Flaccomio, E., Micela, G., & Sciortino, S. 2006, A&A 455, 903
- Nazé, Y., Antokhin, I.I., Rauw, G., Chu, Y.-H., Gosset, E., Vreux, J.-M. 2004, A&A 418, 841
- Nazé, Y., Wang, Q.D., Chu, Y.-H., Gruendl, R., &Oskinova, L. 2014, ApJS 213, 23
- Oey, M.S., & Massey, P. 1995, ApJ 452, 210
- Parker, J.W., Garmany, C.D., Massey, P., & Walborn, N.R. 1992, AJ 103, 1205
- Rosen, A., Lopez, L.A., Krumholz, M.R., Ramirez-Ruiz, E. 2014, MNRAS 442, 2701